


# Optomechanical metamaterial nanobolometer


Cite as: APL Photonics **6**, 126110 (2021); <https://doi.org/10.1063/5.0073583>

Submitted: 01 October 2021 • Accepted: 02 December 2021 • Accepted Manuscript Online: 02 December 2021 • Published Online: 29 December 2021

 Dimitrios Papas,  Jun-Yu Ou,  Eric Plum, et al.

## COLLECTIONS

 This paper was selected as Featured

 This paper was selected as Scilight



View Online



Export Citation



CrossMark

## ARTICLES YOU MAY BE INTERESTED IN

[Machine learning for optical fiber communication systems: An introduction and overview](#)  
APL Photonics **6**, 121101 (2021); <https://doi.org/10.1063/5.0070838>

[Spatio-temporal characterization of ultrashort vector pulses](#)  
APL Photonics **6**, 116103 (2021); <https://doi.org/10.1063/5.0056066>

[An ITO-graphene heterojunction integrated absorption modulator on Si-photonics for neuromorphic nonlinear activation](#)  
APL Photonics **6**, 120801 (2021); <https://doi.org/10.1063/5.0062830>



# Optomechanical metamaterial nanobolometer

Cite as: APL Photon. 6, 126110 (2021); doi: 10.1063/5.0073583

Submitted: 1 October 2021 • Accepted: 2 December 2021 •

Published Online: 29 December 2021



Dimitrios Papas,<sup>1</sup>  Jun-Yu Ou,<sup>1,a)</sup>  Eric Plum,<sup>1,a)</sup>  and Nikolay I. Zheludev<sup>1,2</sup> 

## AFFILIATIONS

<sup>1</sup> Optoelectronics Research Centre and Centre for Photonic Metamaterials, University of Southampton, Highfield, Southampton SO17 1BJ, United Kingdom

<sup>2</sup> Centre for Disruptive Photonic Technologies, SPMS, TPI, Nanyang Technological University, Singapore 637371, Singapore

<sup>a)</sup> Authors to whom correspondence should be addressed: [bruce.ou@soton.ac.uk](mailto:bruce.ou@soton.ac.uk) and [erp@orc.soton.ac.uk](mailto:erp@orc.soton.ac.uk)

## ABSTRACT

Bolometers are detectors of electromagnetic radiation that usually convert the radiation-induced change in temperature of the detector into electric signals. Temperature-dependent electrical resistance in semiconductors and superconductors, the thermoelectric effect in thermocouples, and the pyroelectric effect of transient electric polarization of certain materials when they are heated or cooled are among the underlying physical phenomena used in bolometers. Here, we report that the dependence of the fundamental frequency of a nanowire string detected via scattering of light on the string can be used in a bolometer. Arrays of such nanowires can serve as detectors with high spatial and temporal resolution. We demonstrate a bolometer with 400 nm spatial resolution, 2–3  $\mu$ s thermal response time, and optical power detection noise floor at 3–5 nW/Hz<sup>1/2</sup> at room temperature.

© 2021 Author(s). All article content, except where otherwise noted, is licensed under a Creative Commons Attribution (CC BY) license (<http://creativecommons.org/licenses/by/4.0/>). <https://doi.org/10.1063/5.0073583>

## I. INTRODUCTION

Bolometers detect radiation by measuring temperature increases due to radiation absorption, a principle that is applicable across the electromagnetic spectrum and that permits uncooled detection even of infrared and lower energy radiation. They consist of an absorber and a temperature sensor that are thermally insulated from their surroundings. The radiation-induced temperature change is normally detected electrically as the change in electrical resistance<sup>1,2</sup> through the thermoelectric Seebeck effect<sup>3</sup> or through the pyroelectric effect.<sup>4</sup> Strong temperature-dependence of mechanical resonances of micro- and nanostructures<sup>5–12</sup> has also been exploited to realize nanomechanical bolometers with electromechanical readout,<sup>13–16</sup> while metamaterials have attracted interest as bolometer absorbers with engineered polarization and spectral response.<sup>17–22</sup> Here, we combine nanomechanics and metamaterials to demonstrate an optomechanical metamaterial nanobolometer, where radiation absorption is controlled by the metamaterial design and read optically through light modulation caused by mechanical motion. It exploits the fundamental Brownian motion of nanomechanical oscillators as a signature of temperature. The nanobolometer consists of coupled optical resonators supported by mechanical resonators, which transduce natural sub-nanometer

thermal vibrations to fluctuations of scattered light. The latter reveal the structure's MHz mechanical resonance frequencies that change proportionally to the incident optical power. Our proof-of-principle experiments demonstrate non-contact optical readout with 400 nm spatial resolution, 2–3  $\mu$ s thermal time constants, and nanowatt detectable power based on 2–3%/ $\mu$ W resonance frequency shift per unit of incident optical power (responsivity) with 3–5 nW/Hz<sup>1/2</sup> noise equivalent power in an optomechanical metamaterial nanobolometer of only 100 nm thickness. Advantages of our optically read nanobolometer over prior microbolometer arrays include smaller sensing elements with more than an order of magnitude higher spatial resolution and two orders of magnitude shorter thermal time constant.

## II. CONCEPT AND THEORY

The nanobolometer is based on freestanding nanowires under tensile stress (Fig. 1). Absorption of light by a nanowire increases its temperature, resulting in a stress reduction due to thermal expansion. As in musical strings, lower stress shifts the mechanical resonance of the nanowire to lower frequencies. The natural thermal vibration of the nanowire causes light modulation that reveals its

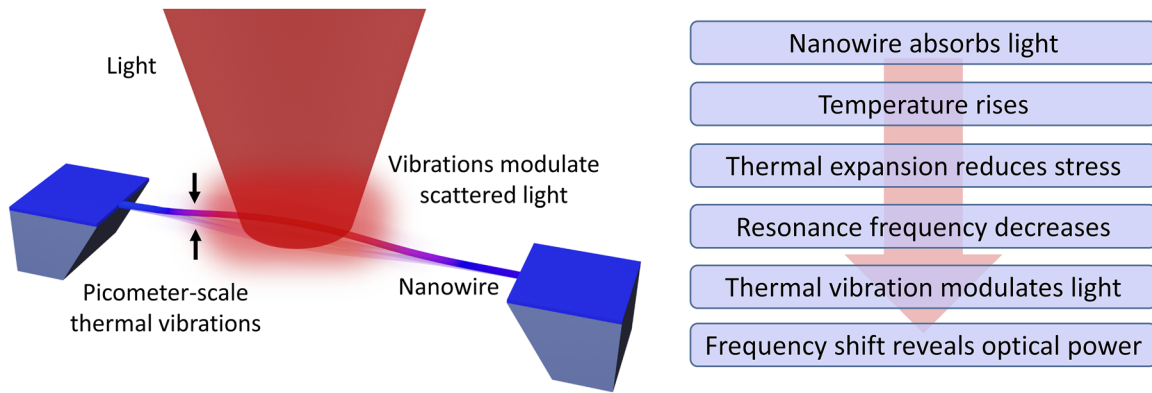


**FIG. 1.** Operating principle of an optomechanical nanowire bolometer. The bolometer is constructed as an array of nanowires. The incident light is partially absorbed by a nanowire (1), its temperature rises (2), and tensile stress along the nanowire is reduced due to thermal expansion (3). The nanowire's mechanical resonance frequency decreases (4). Thermal vibration of the nanowire reveals its resonance frequency through modulation of the scattered light (5), and the frequency variation is used to measure the incident optical power (6).

resonance frequency. The incident optical power is determined from the change in the nanowire's resonance frequency.

According to Euler–Bernoulli beam theory,<sup>23,24</sup> the fundamental resonant frequency  $f_0$  of a doubly clamped nanowire beam (Fig. 1) in the thickness direction is given by

$$f_0(\sigma) = 1.03 \frac{t}{L^2} \sqrt{\frac{E}{\rho}} \sqrt{1 + \frac{\sigma L^2}{3.4Et^2}}, \quad (1)$$

where  $t$  is the thickness,  $L$  is the length,  $E$  is Young's modulus,  $\rho$  is the density of the material, and  $\sigma$  is the tensile stress along the nanowire length. Illumination of the structure leads to optical heating due to absorption, resulting in an average temperature change  $\Delta T$  of the nanowire. The resulting thermal expansion modifies the nanowire's internal stress

$$\sigma = \sigma_0 - \alpha E \Delta T, \quad (2)$$

where  $\sigma_0$  is the initial stress in the nanowire and  $\alpha$  is the nanowire's thermal expansion coefficient. This causes a shift  $\Delta f = f_0(\sigma) - f_0(\sigma_0)$  of the resonance frequency. For small temperature changes, the relative frequency shift is proportional to the temperature change,

$$\frac{\Delta f}{f_0(\sigma_0)} = \beta \Delta T + O(\Delta T^2) \text{ with } \beta = \frac{-\alpha E L^2}{6.8 E t^2 + 2 \sigma_0 L^2}, \quad (3)$$

where  $\beta$  is the linear temperature coefficient of the resonance frequency. The temperature increase  $\Delta T = PA(\lambda)R_{th}$  of the nanowire is determined by the radiation power incident on the nanowire  $P$ , the absorption  $A(\lambda)$  at the wavelength  $\lambda$  of the incident radiation, and the structure's thermal resistance  $R_{th}$ . Therefore, the optical power incident on the nanowire can be measured by determining the frequency shift of its fundamental mechanical resonance. Neglecting higher order terms, the radiation power incident on the nanowire is proportional to its resonance frequency shift,

$$P \approx \frac{1}{\beta A(\lambda) R_{th}} \cdot \frac{\Delta f}{f_0(\sigma_0)}. \quad (4)$$

Combination of such nanowires with optically resonant elements results in a nanomechanical photonic metamaterial supporting optical and mechanical resonances in a single structure of nanoscale thickness. In comparison to the nanowire of Fig. 1, such metamaterials provide an opportunity to control the bolometer's sensitivity to incident radiation and the transduction of thermal motion to modulation of light at the readout wavelength. Spectral and polarization selectivity arise from the metamaterial's resonances of absorption  $A$ . Mechanical resonance frequencies  $f_0$  can be detected by exploiting that, at non-zero temperatures, the natural vibration of mechanical oscillators will be driven by thermal energy.<sup>25–27</sup> In a metamaterial, the thermal motion of metamaterial components will be transduced to modulation of the metamaterial's optical properties. Consider a metamaterial located in the  $xy$ -plane, illuminated by light of intensity  $I_0$ . The dependence of the metamaterial's reflectivity  $R$  on displacement along  $z$  will transduce displacements  $\delta z$  into intensity changes  $\delta I_R$  of the reflected light intensity,

$$\delta I_R = \frac{\partial R(z, \lambda)}{\partial z} \cdot I_0 \delta z. \quad (5)$$

The displacement power spectral density (PSD) for the thermal motion of a mechanical resonator is given by<sup>28</sup>

$$S^2(f) = \frac{(\delta z)^2}{\delta f} = \frac{k_B T f_0}{2\pi^3 m_{\text{eff}} Q [(f_0^2 - f^2)^2 + (ff_0/Q)^2]} \quad (6)$$

for oscillation along  $z$ . Here,  $m_{\text{eff}}$  and  $Q = f_0/\Delta f$  are the effective mass and quality factor of the resonance with spectral width  $\Delta f$ ,  $k_B$  is the Boltzmann constant, and  $T$  is the temperature. Integration over frequency gives the resonator's mean square displacement. Its root mean square (rms) displacement is given by

$$\delta z_{\text{rms}} = \sqrt{\frac{k_B T}{4\pi^2 m_{\text{eff}} f_0^2}}. \quad (7)$$

For a typical silicon nitride metamaterial nanowire of 20  $\mu\text{m}$  length, 250 nm width, 50 nm thickness, and 10 MPa initial stress, we

can expect a resonance frequency  $f_0 = 2.0$  MHz that shifts by  $\beta = 2.3\%/K$  with increasing temperature. Assuming a thermal resistance of  $R_{th} = 5$  K/ $\mu$ W and 50% absorption, this corresponds to a frequency shift of 6%/ $\mu$ W. With a typical quality factor of 1000, such a mechanical resonance would shift by its width in response to 17 nW, implying that power levels of a few nanowatts should be detectable. Such a structure would exhibit thermal displacements of  $\delta z_{rms} = 300$  pm at room temperature, and assuming 1% reflectivity change per nanometer of displacement, this corresponds to rms fluctuations of the absolute reflectivity of  $\frac{\delta I_R}{I_0} = 0.3\%$ .

### III. METAMATERIAL NANOWIRE PAIR NANOBOLOMETER

Initially, we will consider a model system consisting of only two metamaterial nanowires. These are 16  $\mu$ m long and support 14 unit cells. The structure was fabricated by focused ion beam milling (FEI Helios 600 NanoLab) of a 50 nm thick, low stress (<250 MPa), and  $100 \times 100 \mu\text{m}^2$  silicon nitride membrane (Norcada Inc.) coated with 50 nm of thermally evaporated gold [Fig. 2(a)]. The unit cell contains a gold  $\Pi$ -shaped trimer [optical resonator, Fig. 2(b)]. The trimer consists of a larger single nanorod (singlet) and a pair of smaller

nanorods (doublet) that are supported by different silicon nitride nanowires (mechanical resonators).

Such nanowires are the building blocks of a metamaterial that is known to support a Fano resonance.<sup>29,30</sup> The optical properties of the metamaterial were calculated by simulating normal illumination of a single unit cell with periodic boundary conditions (COMSOL 5.3a), describing silicon nitride with a refractive index of 2 and the permittivity of gold by using a Drude-Lorentz model with a plasma frequency of  $1.365 \times 10^{16}$  rad s<sup>-1</sup> and a damping constant of  $3.18 \times 10^{14}$  rad s<sup>-1</sup>. The simulations reveal a plasmonic absorption resonance at about 1250 nm wavelength [Fig. 2(c)]. At this wavelength, the plasmonic trimers operate in a “bright”–“dark” mode configuration<sup>30,31</sup> where a “bright” dipole mode is excited in the larger gold nanorods and an antisymmetric “dark” mode is induced in the pairs of smaller nanorods [Fig. 2(b)]. The metamaterial structure allows for control over the spectral position of its absorption peak through scaling of the unit cell dimensions and offers polarization selectivity (supplementary material, Fig. S1). The motion of one nanowire relative to the other will change the coupling between the plasmonic elements, which leads to a change in their optical properties [Fig. 2(d)]. The sensitivity of the optical properties to displacement can then be controlled by selecting an appropriate readout wavelength. The wavelength of 1310 nm used in our experiments

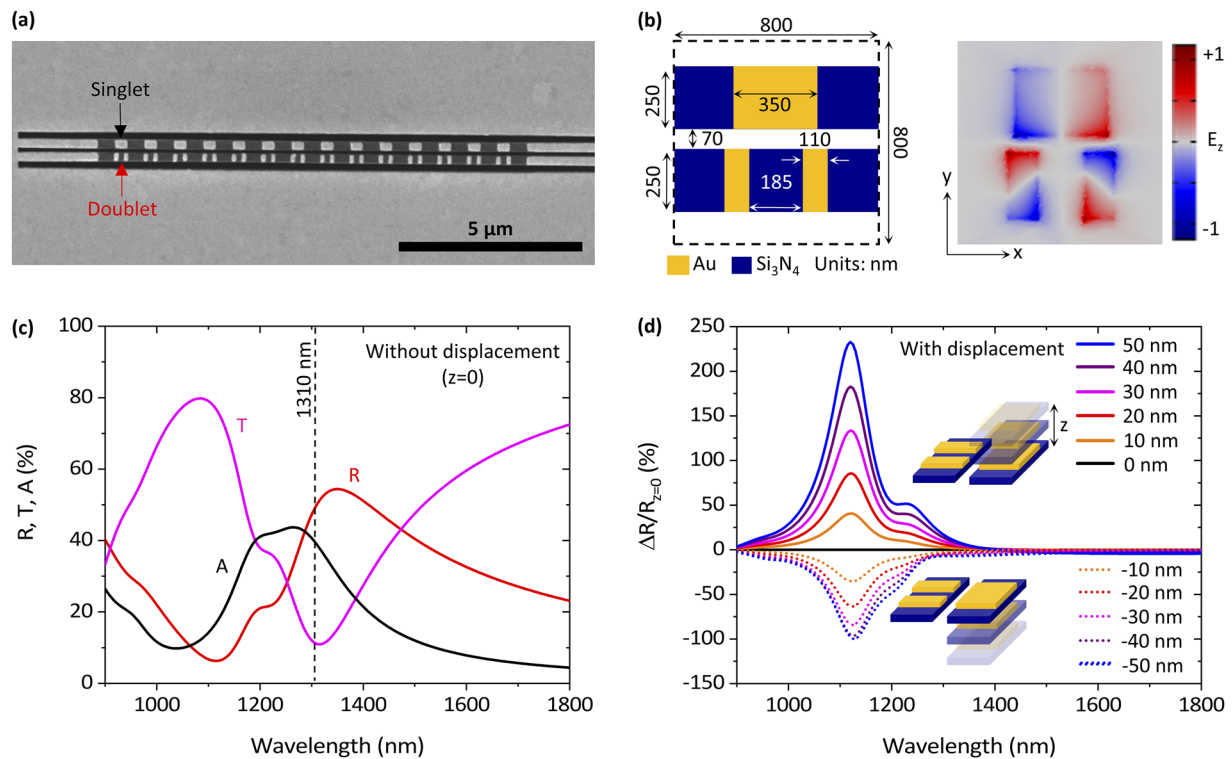


**FIG. 2.** A pair of nanowires as a basic component of the metamaterial bolometer. (a) SEM image of a pair of nanowires supporting singlet and doublet patterns of gold—the building block of a metamaterial. (b) The unit cell of the metamaterial comprising repeated nanowire pairs with dimensions (left). A map of the instantaneous values of the electric field component perpendicular to the plane of the metamaterial, 10 nm above its surface, when the metamaterial is illuminated with light of 1310 nm wavelength (right). (c) Computed reflection (R), transmission (T), and absorption (A) spectra of the metamaterial. (d) Relative reflectivity change  $\Delta R/R_{z=0}$  of the metamaterial array due to mutual out-of-plane displacements  $z$  of the singlet and doublet nanowires. In all cases, incident light is polarized parallel to the nanowires. (Data for illumination with the orthogonal polarization are presented in supplementary material, Fig. S1.)

[Fig. 2(c)] ensures strong absorption and therefore heating of the nanowire structures for thermo-optical control of their fundamental resonances. High reflectivity at this wavelength ensures strong scattering of the incident radiation that can be picked up to detect reflectivity fluctuations of the structure due to thermal motion of its components.

Since our fabricated structure consists of nanowires with varied cross sections, we perform finite element method simulations to calculate the mechanical eigenfrequencies and effective mechanical parameters of the nanowires (COMSOL 5.3a), describing silicon nitride and gold by the properties listed in the [supplementary material](#), Table S1. Without initial tensile stress, the simulated mechanical eigenfrequencies of the fundamental out-of-plane mode of the singlet and doublet nanowires are  $f_0 = 1.481$  and  $1.647$  MHz, respectively. Tensile stress increases these resonance frequencies ([supplementary material](#), Fig. S2). To describe the stress-dependent mechanical eigenfrequencies of the structure analytically, we take each nanowire's effective thickness to be its average thickness and fit the simulations with Eq. (1), arriving at the effective nanowire parameters ( $E$ ,  $\rho$ , and  $t$ ) given in [Table I](#).

To detect the mechanical resonances of the nanowires, we measure the modulation of scattered light caused by their Brownian motion. To avoid damping by air, the sample was placed in a vacuum chamber at a pressure of  $4 \times 10^{-3}$  mbar; see the [supplementary material](#), Fig. S3. A 1310 nm wavelength CW laser beam polarized parallel to the silicon nitride nanowires was focused on the sample (FWHM spot size  $5 \mu\text{m}$  and  $3.5\text{--}70 \mu\text{W}$  total power) with an objective of 0.40 numerical aperture, and the backscattered light was collected and guided to a photodiode (New Focus Inc. 1811). The spectrum of intensity fluctuations, i.e., the optomechanically transduced signal of nanowire motion, was recorded using a spectrum analyzer (Zurich Instruments UHFLI). Considering the spot size and the 800 nm width of the unit cell that contains two nanowires, about 10% of the total incident power illuminates an individual metamaterial nanowire. We take measurements at the center of the structure and detect two resonances around 1.5 and 2 MHz when illuminating each metamaterial nanowire with a few microwatts of laser power [Fig. 3(a)]. The measurements show the power spectral density (PSD) of the backscattered light as a function of frequency and laser power incident on each nanowire. From these measurements, we extract experimental rms displacements<sup>28</sup> of 269 and 249 pm at  $7 \mu\text{W}$  illumination of the singlet and doublet nanowires, respectively. These values are close to the theoretically expected room temperature rms displacements of 274 and 255 pm according to

Eq. (7) based on the observed resonance frequencies and effective masses according to eigenmode simulations ([Table I](#)). A comparison of the observed PSD peaks to the background level indicates a displacement sensitivity<sup>28</sup> of about  $2 \text{ pm/Hz}^{-1/2}$  at the highest incident laser power.

The frequencies of both mechanical resonances decrease linearly with increasing optical power [Figs. 3(a) and 3(b)], as expected according to Eq. (4). Absorption of light increases the nanowire temperatures, reducing their tension by thermal expansion [Eq. (2)], resulting in a decrease in their resonance frequencies [Eq. (3)]. According to a linear fit of the resonance frequencies as a function of power, the singlet and doublet nanowires without illumination resonate at  $f_0(\sigma_0) = 1.592$  and  $2.030$  MHz ([supplementary material](#), Fig. S4). The resonances shift by  $-39$  and  $-58 \text{ kHz}/\mu\text{W}$  of laser power incident on each nanowire, which is a frequency shift of  $-2.4$  and  $-2.8\%/ \mu\text{W}$  and corresponds to the nanobolometer's responsivity. From the variation of detected resonance frequencies at fixed optical power, we determine a frequency noise of  $170 \text{ Hz/Hz}^{1/2}$ , which corresponds to a noise equivalent power of  $4.5$  and  $3.0 \text{ nW/Hz}^{1/2}$ , respectively.

The stress of the nanowires is determined from the observed resonance frequencies using Eq. (1) and the effective nanowire parameters of [Table I](#), and the temperature increase is determined from Eq. (3); see the [supplementary material](#), Fig. S4. The initial tensile stress  $\sigma_0$  is  $2.57$  and  $8.11 \text{ MPa}$  for the singlet and doublet nanowires, their temperature increases by  $1.1$  and  $1.5 \text{ K}/\mu\text{W}$ , and the linear temperature coefficient of the resonance frequency is  $\beta = -2.3$  and  $-1.9\%/ \text{K}$ , respectively. The lower temperature increase in the singlet nanowire is expected as its more extensive gold coverage implies more efficient conductive cooling and thus a lower equilibrium temperature. Considering 37% absorption [[supplementary material](#), Fig. S5(a)], the thermal resistance of the singlet and doublet nanowires is  $R_{\text{th}} = 2.9$  and  $4.0 \text{ K}/\mu\text{W}$ , respectively. With nanowire heat capacities of about  $0.7 \text{ pJ/K}$ , this implies cooling timescales of  $2$  and  $3 \mu\text{s}$ . While the cooling time of the nanomechanical system is only a few microseconds, in practice, the time required for nanobolometer readout will be determined by the measurement of the resonance frequency of a nanowire. Considering the Fourier transform of a time-domain signal, the measurement time required for achieving a frequency resolution that matches the resonance width  $\Delta f$  is  $1/\Delta f$ , which ranges from  $190$  to  $750 \mu\text{s}$  in our nanobolometer. However, both higher accuracy and shorter measurement times may be achieved using frequency interpolation techniques.

We note that the spectral width of the resonances depends on the incident optical power [[supplementary material](#), Fig. S4(c)]. Increasing optical power leads to a decrease in the quality factor of the mechanical resonances from around 1000 at low power to 300–400 at  $7 \mu\text{W}$  per nanowire. This may be due to dissipation dilution, where—at low intensity—the increased tensile stress in the nanomechanical resonators increases the stored vibrational energy relative to the structure's intrinsic losses, resulting in a higher quality factor.<sup>32–34</sup>

#### IV. MECHANICAL METAMATERIAL NANOBOLOMETER

An array of metamaterial nanowires forms a nanomechanical photonic metamaterial, where each nanowire can act as a

**TABLE I.** Effective properties of the two metamaterial nanowires.

	Singlet nanowire	Doublet nanowire
Young's modulus, $E_{\text{eff}}$ (GPa)	227	235
Density, $\rho_{\text{eff}}$ ( $\text{kg m}^{-3}$ )	10 410	7415
Thickness $t_{\text{eff}}$ (nm)	79	73
Thermal expansion coeff. $\alpha_{\text{eff}}$ ( $\text{K}^{-1}$ ) <sup>a</sup>	$4.3 \times 10^{-6}$	$4.0 \times 10^{-6}$
Mass, $m_{\text{eff}}$ (pg)	0.82	0.58
rms displacement, $\delta z_{\text{rms}}$ (pm) at 300 K	274	255

<sup>a</sup>See the [supplementary material](#), Note S1.

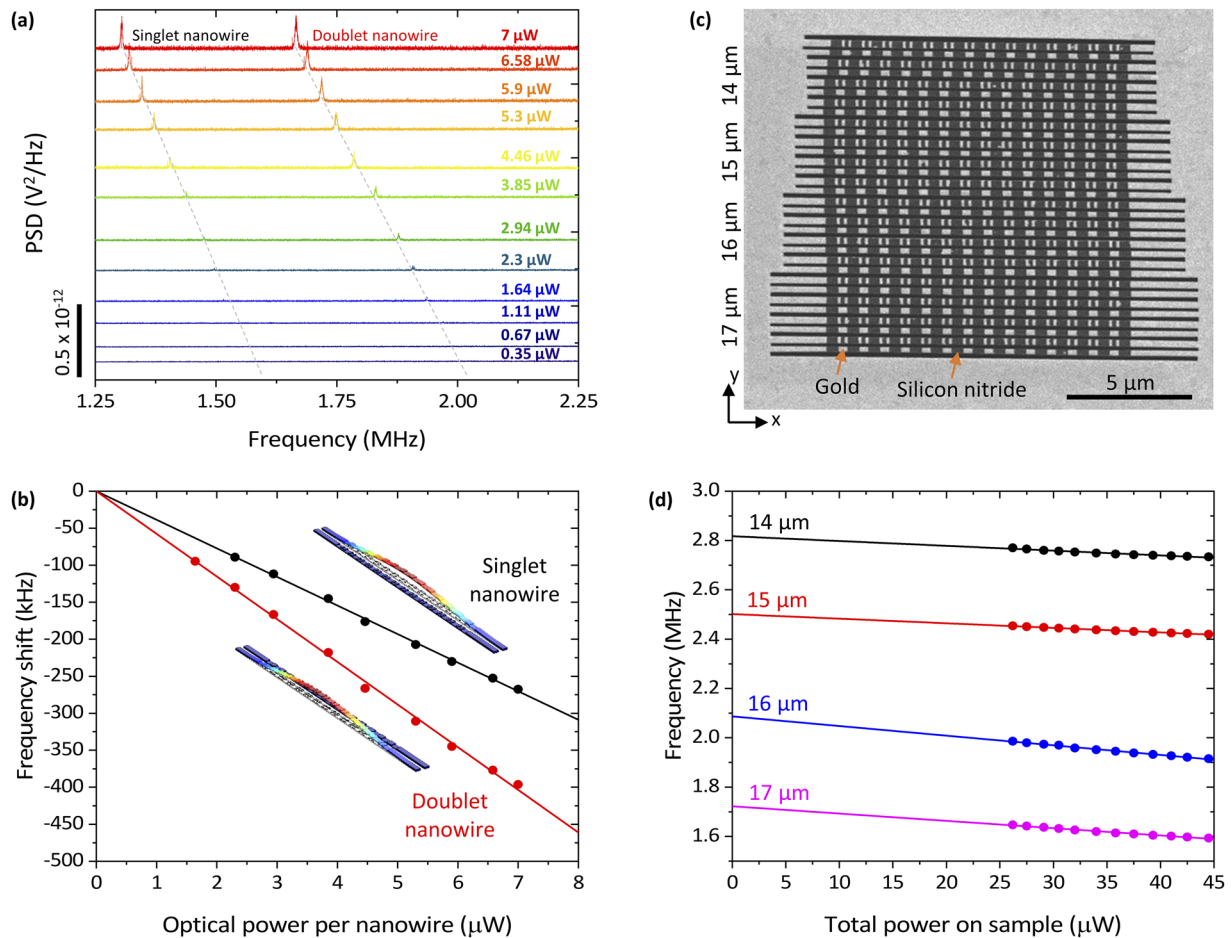


**FIG. 3.** Nano-optomechanical bolometry: power dependence of thermal vibrations of metamaterial nanowires. (a) Power spectral density (PSD) of light scattered by the central part of the nanowire sample for different levels of laser power incident on a nanowire. (b) Shifts of the fundamental mechanical resonance frequencies as functions of incident power per nanowire with linear fits. The insets show the respective mechanical modes for nanowires supporting singlet and doublet plasmonic patterns. (c) SEM image of a nanomechanical metamaterial bolometer array consisting of mechanical resonators of different length. (d) Resonance frequencies, as a function of the total incident optical power, extracted from PSD spectra taken at different positions on the metamaterial sample, with linear fits.

nanobolometer. If these nanowires have sufficiently different mechanical resonance frequencies due to different nanowire lengths or initial stress, then they can be read independently,<sup>35</sup> providing a bolometer array with sub-micrometer spatial resolution. This allows for optical sensing with sub-wavelength spatial resolution or—in principle—polarimetry and spectroscopy based on parallel detection with nanowires supporting optical resonators that absorb different polarization and/or spectral components. To demonstrate this concept, we fabricated an array of metamaterial nanowires [Fig. 3(c)], where we vary the nanowire length from 14 to 17  $\mu\text{m}$  in steps of 1  $\mu\text{m}$ . The metamaterial has an absorption peak close to the measurement wavelength  $\lambda$  of 1310 nm [supplementary material, Fig. S5(a)], as expected from simulations [Fig. 2(c)]. Considering the 800 nm size of the unit cell that contains two nanowires, such structures can provide bolometry with a spatial resolution of about 400 nm, i.e., 0.3  $\lambda$ . We take measurements at four different

positions on the sample, each time focusing on the center of nanowires of a different length. Figure 3(d) shows the dependence of a resonance of each nanowire group on the illumination power. The natural frequency of a nanowire is inversely proportional to the square of its length [Eq. (1)], and therefore, shorter metamaterial nanowires oscillate at higher frequencies. Taking into account that about 10% of the total incident power illuminates a typical nanowire, we observe a responsivity of 1–2%/ $\mu\text{W}$  resonance frequency shift per power incident on a nanowire in the metamaterial. This is slightly lower than for the two beam nanobolometer, which may be due to higher initial stress in the metamaterial sample (supplementary material, Fig. S2). Slightly larger responsivity for longer metamaterial nanowires can be attributed to an increased thermal resistance of the longer nanowires, causing optical heating to slightly higher temperatures.

## V. DISCUSSION

It is interesting to consider how the nanobolometer device might be scaled to other wavelengths. For example, we may scale the lateral dimensions of the entire geometry by a factor  $s$  and keep the thickness constant. Neglecting stress, the mechanical resonance frequency  $f_0$  would scale proportionally to  $s^{-2}$  according to Eq. (1), while the effective mass would scale proportionally to  $s^2$ . Therefore, the thermal rms displacement  $\delta z_{\text{rms}}$  according to Eq. (7) would scale with  $s$ . As the optical resonance wavelength would also scale with  $s$ , this suggests that the magnitude of the rms optical fluctuations would not change much, indicating that the mechanical resonance should remain observable optically. The spatial resolution would scale with  $s$ , i.e., it would remain the same fraction of the wavelength. The thermal resistance  $R_{\text{th}}$  should not change, while the heat capacity and therefore also the cooling timescale would scale with  $s^2$ . The time required to measure the mechanical resonance frequency  $f_0$  of the nanowire also scales with  $s^2$ , indicating that the readout of a significantly larger bolometer would be much slower. The relative frequency shift per Kelvin  $\beta$  should increase for  $s > 1$  according to Eq. (3), implying that the sensing mechanism should scale well to longer wavelengths.

For the proof-of-principle demonstration of the bolometer concept, the nanobolometer measured the power of the same light that was also used for optical readout, resulting in low/high visibility of the mechanical resonances at low/high incident power levels [Fig. 3(a)]. In practical sensor implementations, it would be desirable to use a stable CW laser with fixed power for the optical readout of the sensor to measure the power of a second radiation signal. This would ensure resonance frequency detection with a similar signal-to-noise ratio regardless of the power of the second signal. A readout wavelength closer to 1120 nm [Fig. 2(c)] would maximize the signal-to-noise ratio and allow readout power levels of less than 1  $\mu\text{W}$  per metamaterial nanowire. The sensor's minimum detectable power could be decreased, and the responsivity increased by increasing its thermal resistance, which would be achieved by removing gold from the ends of the metamaterial nanowires.<sup>9</sup> Competition between the increased thermal resistance and a reduced heat capacity would limit the impact on the cooling timescale. Simulations indicate that the reduced effective thickness would yield a decreased mechanical resonance frequency, despite reduced effective density and increased effective Young's modulus. Dielectric metamaterial resonators could be used to achieve higher operational frequencies; more than 100 MHz have been reported.<sup>36</sup> More generally, the spectral and polarization sensitivity, as well as the transduction of thermal vibrations to modulation of light at the readout wavelength, can be engineered by the metamaterial design, and detailed mechanical characterization of such structures can be performed by hyperspectral motion visualization scanning electron microscopy (SEM).<sup>37</sup>

In comparison to nanoelectromechanical,<sup>13,38</sup> metamaterial,<sup>20–22</sup> and conventional<sup>39,40</sup> microbolometer arrays, our optically read nanobolometer structures offer smaller sensing elements (4  $\mu\text{m}^2$ ) with more than an order of magnitude better spatial resolution (400 nm) and two orders of magnitude shorter thermal time constant. In contrast, single-pixel microbolometers,<sup>14–18</sup> as well as nanobolometers fed by microscale or larger antennas,<sup>41,42</sup> do not offer nanoscale resolution.

The dependence of mechanical resonances of nanomechanical photonic metamaterials on optical power also provides an opportunity for tuning of giant electro-optical,<sup>43</sup> magneto-optical,<sup>44</sup> acousto-optical,<sup>45</sup> and nonlinear<sup>29,35,36</sup> optical effects, which have been observed in such nanostructures. At natural resonances, mechanical oscillations can be driven to big amplitudes, resulting in large modulation of optical properties around the optical resonances of the metamaterial. Optical control of mechanical resonances, therefore, provides dynamic control over the natural frequencies at which efficient light modulation can be achieved. Our results show that frequencies and quality factors of natural mechanical resonances of nanomechanical photonic metamaterials can be continuously tuned by optical heating affecting mechanical tension in the nanostructure. We observe frequency shifts of up to 20% and Q-factor changes of up to 300% at optical power levels of few microwatts per metamaterial nanowire. Such tuning may also be applied to photonic metamaterials with addressable mechanical elements for applications such as dynamic diffraction gratings,<sup>46</sup> subwavelength resolution spatial light modulators,<sup>35</sup> light modulation, temperature sensing, spectroscopy, imaging, and the study of coupled mechanical systems.<sup>47</sup>

## VI. CONCLUSIONS

In conclusion, we demonstrate a mechanical metamaterial nanobolometer with a non-contact optical readout. The nanobolometer is based on detecting the modulation of light caused by the fundamental sub-nanometer Brownian oscillation of a nanomechanical photonic metamaterial. The thermal motion of the metamaterial's mechanical oscillators modulates the relative position of the structure's coupled plasmonic resonators by 100s of picometers, causing detectable intensity modulation of light scattered by the nanostructure. Plasmonic absorption, and thus, heating of the structure result in internal tensile stress variations that modify the mechanical resonance frequencies of individual mechanical elements by 2–3%/ $\mu\text{W}$  of incident power. Such bolometers offer sub-micrometer spatial resolution, microsecond response times, and nanowatt detection.

## SUPPLEMENTARY MATERIAL

See the [supplementary material](#) for material properties of silicon nitride and gold used in our calculations, more details on the metamaterial's optical properties, stress-dependent eigenfrequency simulations, a schematic of the experimental setup, and the optical power dependence of resonances and temperature of metamaterial nanowires.

## ACKNOWLEDGMENTS

This work was supported by the UK's Engineering and Physical Sciences Research Council (Grant Nos. EP/M009122/1 and EP/T02643X/1), the Singapore Ministry of Education [Grant No. MOE2016-T3-1-006 (S)], and the Office of Naval Research (Grant No. N62909-18-1-2026).

## AUTHOR DECLARATIONS

### Conflict of Interest

The authors have no conflicts to disclose.

## DATA AVAILABILITY

The data that support the findings of this study are openly available in the University of Southampton ePrints research repository at <https://doi.org/10.5258/SOTON/D1961>.<sup>48</sup>

## REFERENCES

- <sup>1</sup>P. L. Richards, "Bolometers for infrared and millimeter waves," *J. Appl. Phys.* **76**, 1–24 (1994).
- <sup>2</sup>A. Shurakov, Y. Lobanov, and G. Goltsman, "Superconducting hot-electron bolometer: From the discovery of hot-electron phenomena to practical applications," *Supercond. Sci. Technol.* **29**, 023001 (2015).
- <sup>3</sup>A. Varpula, K. Tappura, J. Tiira, K. Grigoros, O.-P. Kilpi, K. Sovanto, J. Ahopelto, and M. Prunnila, "Nano-thermoelectric infrared bolometers," *APL Photonics* **6**, 036111 (2021).
- <sup>4</sup>U. Sassi, R. Parret, S. Nanot, M. Bruna, S. Borini, D. De Fazio, Z. Zhao, E. Lidorikis, F. H. L. Koppens, A. C. Ferrari, and A. Colli, "Graphene-based mid-infrared room-temperature pyroelectric bolometers with ultrahigh temperature coefficient of resistance," *Nat. Commun.* **8**, 14311 (2017).
- <sup>5</sup>V. Pini, J. Tamayo, E. Gil-Santos, D. Ramos, P. Kosaka, H.-D. Tong, C. van Rijn, and M. Calleja, "Shedding light on axial stress effect on resonance frequencies of nanocantilevers," *ACS Nano* **5**, 4269–4275 (2011).
- <sup>6</sup>T. Larsen, S. Schmid, L. Grönberg, A. O. Niskanen, J. Hassel, S. Dohn, and A. Boisen, "Ultrasensitive string-based temperature sensors," *Appl. Phys. Lett.* **98**, 121901 (2011).
- <sup>7</sup>X. C. Zhang, E. B. Myers, J. E. Sader, and M. L. Roukes, "Nanomechanical torsional resonators for frequency-shift infrared thermal sensing," *Nano Lett.* **13**, 1528–1534 (2013).
- <sup>8</sup>T. Larsen, S. Schmid, L. G. Villanueva, and A. Boisen, "Photothermal analysis of individual nanoparticulate samples using micromechanical resonators," *ACS Nano* **7**, 6188–6193 (2013).
- <sup>9</sup>S. Schmid, K. Wu, P. E. Larsen, T. Rindzevicius, and A. Boisen, "Low-power photothermal probing of single plasmonic nanostructures with nanomechanical string resonators," *Nano Lett.* **14**, 2318–2321 (2014).
- <sup>10</sup>R. Thijssen, T. J. Kippenberg, A. Polman, and E. Verhagen, "Parallel transduction of nanomechanical motion using plasmonic resonators," *ACS Photonics* **1**, 1181–1188 (2014).
- <sup>11</sup>F. Yi, H. Zhu, J. C. Reed, and E. Cubukcu, "Plasmonically enhanced thermomechanical detection of infrared radiation," *Nano Lett.* **13**, 1638–1643 (2013).
- <sup>12</sup>L. Vicarelli, A. Tredicucci, and A. Pitanti, "Micromechanical bolometers for sub-terahertz detection at room temperature," *arXiv:2107.12170* [physics.ins-det] (2021).
- <sup>13</sup>L. Laurent, J.-J. Yon, J.-S. Moulet, M. Roukes, and L. Durauffourg, "12  $\mu\text{m}$ -pitch electromechanical resonator for thermal sensing," *Phys. Rev. Appl.* **9**, 024016 (2018).
- <sup>14</sup>Y. Hui, J. S. Gomez-Diaz, Z. Qian, A. Alù, and M. Rinaldi, "Plasmonic piezoelectric nanomechanical resonator for spectrally selective infrared sensing," *Nat. Commun.* **7**, 11249 (2016).
- <sup>15</sup>A. Blaikie, D. Miller, and B. J. Alemán, "A fast and sensitive room-temperature graphene nanomechanical bolometer," *Nat. Commun.* **10**, 4726 (2019).
- <sup>16</sup>Z. Qian, V. Rajaram, S. Kang, and M. Rinaldi, "High figure-of-merit nems thermal detectors based on 50-nm thick aln nano-plate resonators," *Appl. Phys. Lett.* **115**, 261102 (2019).
- <sup>17</sup>Y. Kim, D. Kim, S.-H. Lee, M. Seo, H.-J. Jung, B. Kang, S.-M. Lee, and H.-J. Lee, "Single-layer metamaterial bolometer for sensitive detection of low-power terahertz waves at room temperature," *Opt. Express* **28**, 17143 (2020).
- <sup>18</sup>F. B. P. Niesler, J. K. Gansel, S. Fischbach, and M. Wegener, "Metamaterial metal-based bolometers," *Appl. Phys. Lett.* **100**, 203508 (2012).
- <sup>19</sup>V. Savinov, V. A. Fedotov, P. A. J. de Groot, and N. I. Zheludev, "Radiation-harvesting resonant superconducting sub-THz metamaterial bolometer," *Supercond. Sci. Technol.* **26**, 084001 (2013).
- <sup>20</sup>H. Tao, E. A. Kadlec, A. C. Strikwerda, K. Fan, W. J. Padilla, R. D. Averitt, E. A. Shaner, and X. Zhang, "Microwave and terahertz wave sensing with metamaterials," *Opt. Express* **19**, 21620–21626 (2011).
- <sup>21</sup>J. Grant, I. Escorcia-Carranza, C. Li, I. J. H. McCrindle, J. Gough, and D. R. S. Cumming, "A monolithic resonant terahertz sensor element comprising a metamaterial absorber and micro-bolometer," *Laser Photonics Rev.* **7**, 1043 (2013).
- <sup>22</sup>I. E. Carranza, J. Grant, J. Gough, and D. R. S. Cumming, "Metamaterial-based terahertz imaging," *IEEE Trans. Terahertz Sci. Technol.* **5**, 892 (2015).
- <sup>23</sup>A. Bokaian, "Natural frequencies of beams under tensile axial loads," *J. Sound Vib.* **142**, 481–498 (1990).
- <sup>24</sup>S. C. Jun, X. M. H. Huang, M. Manolidis, C. A. Zorman, M. Mehregany, and J. Hone, "Electrothermal tuning of Al-SiC nanomechanical resonators," *Nanotechnology* **17**, 1506–1511 (2006).
- <sup>25</sup>R. Thijssen, T. J. Kippenberg, A. Polman, and E. Verhagen, "Plasmomechanical resonators based on dimer nanoantennas," *Nano Lett.* **15**, 3971–3976 (2015).
- <sup>26</sup>R. Thijssen, E. Verhagen, T. J. Kippenberg, and A. Polman, "Plasmon nanomechanical coupling for nanoscale transduction," *Nano Lett.* **13**, 3293–3297 (2013).
- <sup>27</sup>B. J. Roxworthy and V. A. Aksyuk, "Nanomechanical motion transduction with a scalable localized gap plasmon architecture," *Nat. Commun.* **7**, 13746 (2016).
- <sup>28</sup>B. D. Hauer, C. Doolin, K. S. D. Beach, and J. P. Davis, "A general procedure for thermomechanical calibration of nano/micro-mechanical resonators," *Ann. Phys.* **339**, 181–207 (2013).
- <sup>29</sup>J.-Y. Ou, E. Plum, J. Zhang, and N. I. Zheludev, "Giant nonlinearity of an optically reconfigurable plasmonic metamaterial," *Adv. Mater.* **28**, 729–733 (2016).
- <sup>30</sup>S. Zhang, D. A. Genov, Y. Wang, M. Liu, and X. Zhang, "Plasmon-induced transparency in metamaterials," *Phys. Rev. Lett.* **101**, 047401 (2008).
- <sup>31</sup>N. Liu, L. Langguth, T. Weiss, J. Kästel, M. Fleischhauer, T. Pfau, and H. Giessen, "Plasmonic analogue of electromagnetically induced transparency at the Drude damping limit," *Nat. Mater.* **8**, 758–762 (2009).
- <sup>32</sup>Q. P. Unterreithmeier, T. Faust, and J. P. Kotthaus, "Damping of nanomechanical resonators," *Phys. Rev. Lett.* **105**, 027205 (2010).
- <sup>33</sup>S. A. Fedorov, N. J. Engelsens, A. H. Ghadimi, M. J. Bereyhi, R. Schilling, D. J. Wilson, and T. J. Kippenberg, "Generalized dissipation dilution in strained mechanical resonators," *Phys. Rev. B* **99**, 054107 (2019).
- <sup>34</sup>S. Verbridge, D. F. Shapiro, H. G. Craighead, and J. M. Parpia, "Macroscopic tuning of nanomechanics: Substrate bending for reversible control of frequency and quality factor of nanostring resonators," *Nano Lett.* **7**, 1728–1735 (2007).
- <sup>35</sup>J.-Y. Ou, E. Plum, and N. I. Zheludev, "Optical addressing of nanomechanical metamaterials with subwavelength resolution," *Appl. Phys. Lett.* **113**, 081104 (2018).
- <sup>36</sup>A. Karvounis, J.-Y. Ou, W. Wu, K. F. MacDonald, and N. I. Zheludev, "Nano-optomechanical nonlinear dielectric metamaterials," *Appl. Phys. Lett.* **107**, 191110 (2015).
- <sup>37</sup>T. Liu, J.-Y. Ou, E. Plum, K. F. MacDonald, and N. I. Zheludev, "Visualization of subatomic movements in nanostructures," *Nano Lett.* **21**, 7746–7752 (2021).
- <sup>38</sup>F. Niklaus, C. Vieider, and H. Jakobsen, "MEMS-based uncooled infrared bolometer arrays: A review," *Proc. SPIE* **6836**, 68360D (2008).
- <sup>39</sup>G. D. Skidmore, C. J. Han, and C. Li, "Uncooled microbolometers at DRS and elsewhere through 2013," *Proc. SPIE* **9100**, 910003 (2014).
- <sup>40</sup>M. Y. Tanrikulu, Ç. Yildizak, A. K. Okyay, O. Akar, A. Saraç, and T. Akin, "Realization of single layer microbolometer detector pixel using ZnO material," *IEEE Sens. J.* **20**, 9677 (2020).
- <sup>41</sup>R. Kokkonen, J. Govenius, V. Vesterinen, R. E. Lake, A. M. Gunyhó, K. Y. Tan, S. Simbierowicz, L. Grönberg, J. Lehtinen, M. Prunnila, J. Hassel, A. Lamminen, O.-P. Saira, and M. Möttönen, "Nanobolometer with ultralow noise equivalent power," *Commun. Phys.* **2**, 124 (2019).
- <sup>42</sup>H.-H. Yang, "Sub-10 pW/Hz<sup>0.5</sup> room temperature Ni nano-bolometer," *Appl. Phys. Lett.* **108**, 053106 (2016).

- <sup>43</sup>J.-Y. Ou, E. Plum, J. Zhang, and N. I. Zheludev, “An electromechanically reconfigurable plasmonic metamaterial operating in the near-infrared,” *Nat. Nanotechnol.* **8**, 252–255 (2013).
- <sup>44</sup>J. Valente, J.-Y. Ou, E. Plum, I. J. Youngs, and N. I. Zheludev, “A magneto-electro-optical effect in a plasmonic nanowire material,” *Nat. Commun.* **6**, 7021 (2015).
- <sup>45</sup>D. Papas, J. Y. Ou, E. Plum, and N. I. Zheludev, “Acoustically driven photonic metamaterials,” in *Nanometa*, Seefeld, Austria (2019).
- <sup>46</sup>P. Cencillo-Abad, E. Plum, E. T. F. Rogers, and N. I. Zheludev, “Spatial optical phase-modulating metadvice with subwavelength pixelation,” *Opt. Express* **24**, 18790–18798 (2016).
- <sup>47</sup>H. Okamoto, R. Schilling, H. Schütz, V. Sudhir, D. J. Wilson, H. Yamaguchi, and T. J. Kippenberg, “A strongly coupled  $\Lambda$ -type micromechanical system,” *Appl. Phys. Lett.* **108**, 153105 (2016).
- <sup>48</sup>D. Papas, J. Y. Ou, E. Plum, and N. I. Zheludev (2021). “Dataset for optomechanical metamaterial nanobolometer,” University of Southampton ePrints Research Repository. <https://doi.org/10.5258/SOTON/D1961>